

*This copy is for your personal, non-commercial use only.*

If you wish to distribute this article to others, you can order high-quality copies for your colleagues, clients, or customers by [clicking here](#).

Permission to republish or repurpose articles or portions of articles can be obtained by following the guidelines [here](#).

**The following resources related to this article are available online at [www.sciencemag.org](http://www.sciencemag.org) (this information is current as of June 8, 2010 ):**

**Updated information and services**, including high-resolution figures, can be found in the online version of this article at:

<http://www.sciencemag.org/cgi/content/full/288/5471/1624>

This article **cites 20 articles**, 3 of which can be accessed for free:

<http://www.sciencemag.org/cgi/content/full/288/5471/1624#otherarticles>

This article has been **cited by** 439 article(s) on the ISI Web of Science.

This article has been **cited by** 8 articles hosted by HighWire Press; see:

<http://www.sciencemag.org/cgi/content/full/288/5471/1624#otherarticles>

This article appears in the following **subject collections**:

Chemistry

<http://www.sciencemag.org/cgi/collection/chemistry>

# Light-Driven Motion of Liquids on a Photoresponsive Surface

Kunihiro Ichimura,\* Sang-Keun Oh, Masaru Nakagawa

The macroscopic motion of liquids on a flat solid surface was manipulated reversibly by photoirradiation of a photoisomerizable monolayer covering the surface. When a liquid droplet several millimeters in diameter was placed on a substrate surface modified with a calix[4]resorcinarene derivative having photochromic azobenzene units, asymmetrical photoirradiation caused a gradient in surface free energy due to the photoisomerization of surface azobenzenes, leading to the directional motion of the droplet. The direction and velocity of the motion were tunable by varying the direction and steepness of the gradient in light intensity. The light-driven motion of a fluid substance in a surface-modified glass tube suggests potential applicability to microscale chemical process systems.

A gradient in surface tension can induce a net mass transport of liquids, which affords a driving force for the operation of microfluidic devices (1) and for biological cell motility in vitro (2, 3). Such nonmechanical flow arising from the action of a surface tension gradient can be created by several approaches, including thermal (4), chemical (5), and electrochemical (6) methods. Because the surface free energies of flat solid substrates are determined by atomic-level constitutions of their outermost surfaces (7, 8), the alteration of chemical structures of the outermost monomolecular layers by light (or some other external stimulus) can be used to trigger and manipulate various interfacial phenomena, including wettability (9, 10), liquid crystal alignment (11, 12), and dispersibility (13). Thus, if a gradient in surface energy is generated photochemically as a result of spatially controlled changes of chemical structures of an outermost surface, the motion of a liquid can be guided by spatially controlled photoirradiation of the photoresponsive substrate surface on which the liquid is placed. We now report that the motion of liquids can be manipulated reversibly by light when a substrate surface is modified with a photoisomerizable azobenzene monolayer. The light-driven motion of liquids (14) is achieved by an appropriate choice of photoreactive molecules tethered to an outermost surface and fluid substances.

We used here a crown conformer of *O*-carboxymethylated calix[4]resorcinarene (CRA-CM, Fig. 1) bearing four *p*-octylazobenzene residues at one of the rims of the cyclic skeleton (15) to assemble a photoresponsive monolayer. CRA-CM as a macrocyclic amphiphile was designed to ensure a sufficient free volume required for trans-to-cis photoisomerization of the azobenzene moieties, even if the cyclic

skeletons of CRA-CM form a densely packed monolayer (16). This situation arises because the molecular packing is determined specifically by the rigid cylindrical macrocycle. The photoresponsive self-assembled monolayer was prepared simply by immersing an aminosilylated silica plate in a dilute solution of CRA-CM, yielding a robust monolayer with dense packing (15). As a result of the flat-laid adsorption of CRA-CM molecules on a silica surface (17), we anticipated that the octylazobenzene units in their trans state would be stretched out to be exposed to the air. Ultraviolet (UV)-visible spectral measurements revealed that photoirradiation of the monolayer with UV (365 nm) light results in the formation of ~90% of cis isomer with a higher dipole moment; hence, the outermost surface of a UV-exposed CRA-CM monolayer is likely terminated by the polar cis-azo groups, leading to an increase in surface free energy. Photoirradiation of the cis-rich surface with blue (436 nm) light causes the cis isomer to reverse into the trans isomer.

To investigate the light-guided movement of a droplet of olive oil (18), we placed the droplet on the photoresponsive surface of the CRA-CM-modified plate and then used spatially controlled irradiation to generate a gradient in the level of photoisomerization. Figure 2 shows the directional motion of a droplet on a cis-rich surface upon asymmetrical irradiation with blue light. We used the edge of a focused light beam from a Xe-Hg lamp to produce irradiation that was asymmetrical in its intensity. The surface energy gradient between the advancing and receding edges of the droplet was constantly maintained by moving the light beam, which continued moving the droplet. Thus, there is no theoretical limitation in moving distance for this photochemical method. To stop the movement of the droplet, we irradiated the photoresponsive surface with a homogeneous blue light (Fig. 2C). The velocity of the droplet intrinsically relied on the intensity and gradient of the light. A typical speed of 35  $\mu\text{m/s}$  was observed

for the motion of a ~2- $\mu\text{l}$  droplet of olive oil.

To evaluate the effect of liquid-solid interfacial interactions on the light-guided motion, we measured advancing ( $\theta_{\text{adv}}$ ) and receding ( $\theta_{\text{rec}}$ ) contact angles for various liquids on the surface-modified plate before and after UV light irradiation (Table 1). No motion of droplets on the surface-modified plate was generated by the photoirradiation for some liquids shown in Table 1, even though their  $\theta_{\text{adv}}$  and  $\theta_{\text{rec}}$  were altered after illumination with UV light. Changes in equilibrium thermodynamic properties such as  $\theta_{\text{adv}}$  provide an essential driving force for the motion to occur. The motion of liquid on a solid substrate, however, is primarily governed by dynamic factors such as the ability of the surface molecules to be reorganized within the experimental time scale. Consequently, the motion of the liquids exhibiting large contact angle hystereses ( $\Delta\theta = \theta_{\text{adv}} - \theta_{\text{rec}}$ ), which are likely to be attributable to the reorganization of surface molecules (19), may be restricted. Taking into account these results, we suggest that the motion of a droplet requires the condition that  $\theta_{\text{rec}}$  for the trans isomer ( $\theta_{\text{rec}}^{\text{tr}}$ ) be larger than  $\theta_{\text{adv}}$  for the cis isomer ( $\theta_{\text{adv}}^{\text{cis}}$ ) (20). The surface-assisted motion was workable for 1-methylnaphthalene and 1,1,2,2-tetrachloroethane, and even for nematic liquid crystals including NPC-02 (a binary mixture of 4-propyl-4'-ethoxy- and 4-propyl-4'-butoxyphenylcyclohexanes) and 5CB (4-pentyl-4'-cyanobiphenyl), because they all fulfill the requirement  $\theta_{\text{rec}}^{\text{tr}} > \theta_{\text{adv}}^{\text{cis}}$  (Table 1). Note that NPC-02, relative to common organic liquids, exhibits both smaller hysteresis and larger photoinduced changes in contact angles (21) upon photoisomerization, so that NPC-02 is quite suitable for quantitative interpretation of the light-driven motion.

Alternating irradiation of a CRA-CM monolayer with homogeneous UV and blue light (1.0  $\text{mW cm}^{-2}$ , 100 s) led to reversible in situ symmetrical spreading and dewetting of droplets of the liquids exhibiting  $\theta_{\text{rec}}^{\text{tr}} > \theta_{\text{adv}}^{\text{cis}}$ . Figure 3 illustrates the correlation between the level of cis isomer and the diameter of an NPC-02 droplet on the plate during the alternating irradiation.

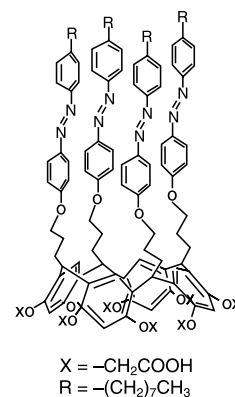
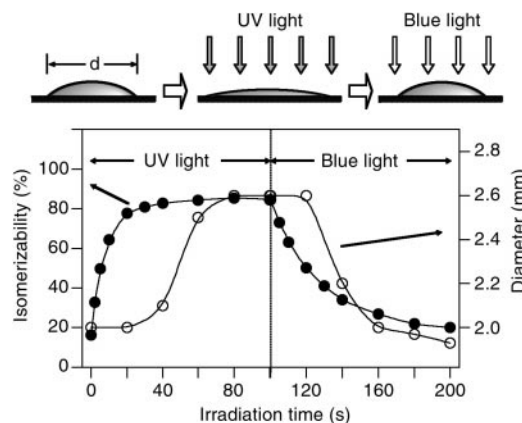
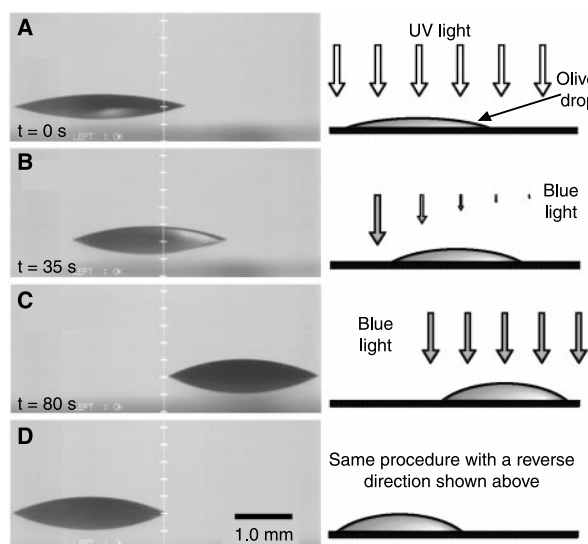


Fig. 1. Macrocyclic amphiphile tethering photochromic azobenzene units (CRA-CM).

Chemical Resources Laboratory, Tokyo Institute of Technology, 4259 Nagatsuta, Midori-ku, Yokohama 226-8503, Japan.

\*To whom correspondence should be addressed. E-mail: kichimur@res.titech.ac.jp



**Fig. 2 (left).** Lateral photographs of light-driven motion of an olive oil droplet on a silica plate modified with CRA-CM. The olive oil droplet on a cis-rich surface moved in a direction of higher surface energy by asymmetrical irradiation with 436-nm light perpendicular to the surface. (A to C) The sessile contact angles were changed from 18° (A) to 25° (C). (D) The moving direction of the droplet was controllable by

varying the direction of the photoirradiation.

**Fig. 3 (right).** Correlation between the level of cis isomer (solid circles) and the diameter (open circles) of an NPC-02 droplet placed on a silica plate modified with CRA-CM upon homogeneous irradiation with UV and blue light (1.0 mW cm<sup>-2</sup>). The level of photoisomerization was estimated by monitoring the UV-visible absorption spectrum of the plate. The viscosity of NPC-02 is 9.8 mPa s at 23°C. The sessile contact angles before and after UV irradiation were 24° and 11°, respectively.

Note that the spreading is delayed markedly when compared with the photoisomerization processes; the droplet starts to spread after the trans-to-cis conversion is almost accomplished under UV irradiation. The delay in the deformation of the droplet shape likely arises from dynamic processes involving the reorientation of photoisomerized azobenzenes so as to minimize an interfacial energy (22, 23). This effect should be one of the factors affecting the velocity of a light-driven motion of a liquid droplet (Fig. 2) in addition to the steepness of the gradient in surface energy, the droplet volume, and the surface tension and viscosity of the droplet (5).

The time evolution of the directional motion of an NPC-02 droplet on a cis-rich surface by asymmetrical irradiation with blue light was

investigated. As shown in Fig. 4, the advancing front of the droplet did not move at all in the early stage of the irradiation for about 20 s, although the diameter of the droplet decreased markedly. This dewetting caused an increase in contact angles of both advancing and receding edges of the droplet, because the pressure inside the droplet equilibrates rapidly (24). After the initial induction time, the droplet started to move at a dynamic contact angle of about 20°, which was retained during the motion. The observation clearly supports the idea that the driving force for the light-driven liquid motion is an imbalance in contact angles generated on both edges of a droplet, because the dynamic contact angle exhibits an intermediate value between  $\theta_{adv}^{cis}$  and  $\theta_{rec}^{tr}$  (5, 25).

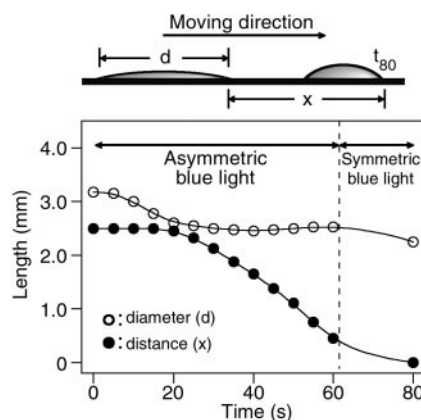


**Fig. 4.** Changes in position and diameter of the moving NPC-02 droplet on a CRA-CM-modified plate as a function of time. Photoirradiation of the plate was carried out by the same procedure shown in Fig. 2. A speed of 50  $\mu$ m/s was observed for the motion of a  $\sim$ 2- $\mu$ m droplet.

No deterioration was observed even after more than 100 cycles of the light-driven motions. We conducted two additional experiments that reveal distinctive features of this photochemical method to position liquids. First, when an NPC-02 droplet was exposed to alternating irradiation with asymmetrical UV and blue light, the droplet migrated stepwise to capture a glass bead 0.5 mm in diameter (Fig. 5). It was possible to convey the bead by the spatially controlled alternating irradiation. Second, the migration of NPC-02 placed in a glass tube, the inside wall of which was modified with the CRA-CM in advance, was controllable by the asymmetrical irradiation (Fig. 6).

Because photochemical events can be controlled precisely in time and space, the surface-assisted, light-driven motion of liquids should lead to improved understanding of interface phenomena, including the spreading kinetics and the role of surface tension gradients.

**Table 1.** Contact angles of CRA-CM monolayer for various liquids. The values were within experimental error of  $\pm 2^\circ$ .

Probe liquid	Angle ( $^\circ$ )			
	Trans isomer		Cis isomer	
	$\theta_{adv}$	$\theta_{rec}$	$\theta_{adv}$	$\theta_{rec}$
<i>No motion</i>				
Water	94	40	86	51
Formamide	68	17	62	19
Ethylene glycol	61	36	56	39
Poly(ethylene glycol)*	42	37	38	31
<i>Motion</i>				
1-Methylnaphthalene	26	24	20	18
1,1,2,2-Tetrachloroethane	18	16	12	11
5CB	43	37	22	19
NPC-02	28	24	11	10
Olive oil	29	25	17	13

\*Average molecular weight was 400.

## References and Notes

1. M. Grunze, *Science* **283**, 41 (1999).
2. S. B. Carter, *Nature* **213**, 256 (1967).
3. —, *Nature* **208**, 1183 (1965).
4. A. M. Cazabat, F. Heslot, S. M. Troian, P. Carles, *Nature* **346**, 824 (1990).
5. M. K. Chaudhury and G. M. Whitesides, *Science* **256**, 1539 (1992).
6. B. S. Gallardo et al., *Science* **283**, 57 (1999).
7. G. M. Whitesides and P. E. Laibinis, *Langmuir* **6**, 87 (1990).
8. C. D. Bain and G. M. Whitesides, *Angew. Chem. Int. Ed. Engl.* **28**, 506 (1989).
9. L. M. Siewierski, W. J. Brittain, S. Petrasch, M. D. Foster, *Langmuir* **12**, 5838 (1996).
10. G. Möller, M. Harke, H. Motschmann, D. Prescher, *Langmuir* **14**, 4955 (1998).
11. K. Ichimura, Y. Suzuki, T. Seki, A. Hosoki, K. Aoki, *Langmuir* **4**, 1214 (1988).
12. K. Ichimura, *Chem. Rev.*, in press.
13. M. Ueda, H.-B. Kim, K. Ichimura, *J. Mater. Chem.* **4**, 883 (1994).
14. Abbott and co-workers have reported that release of droplets of aqueous solutions of azobenzene-con-

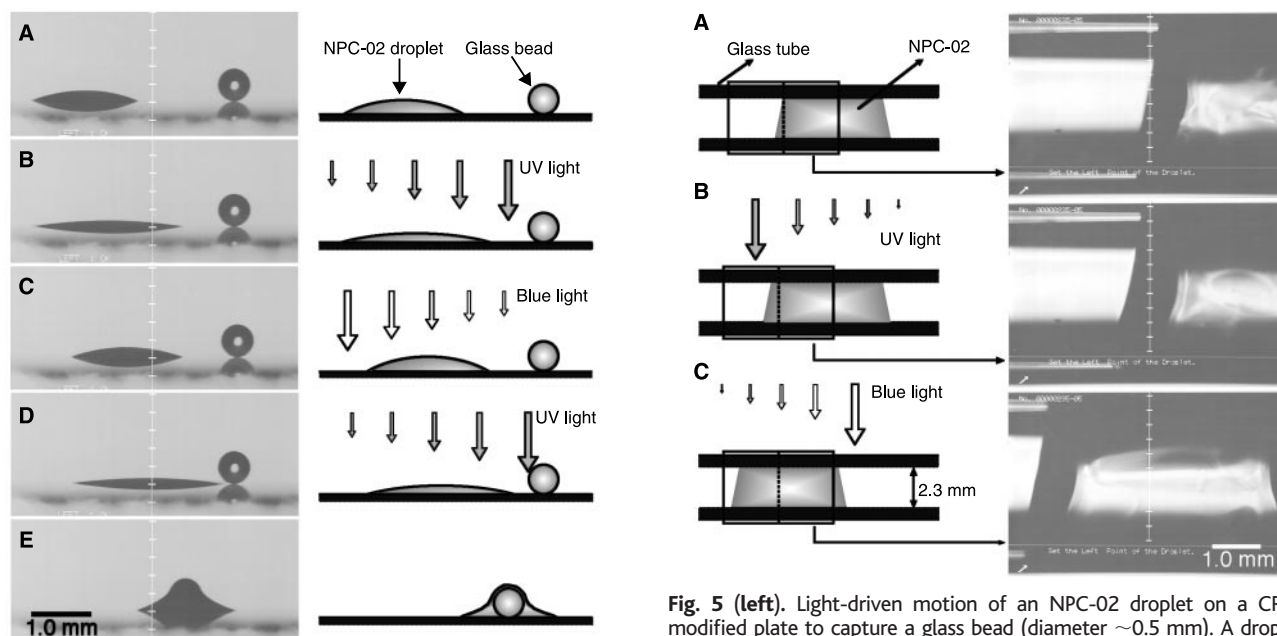


**Fig. 5 (left).** Light-driven motion of an NPC-02 droplet on a CRA-CM-modified plate to capture a glass bead (diameter  $\sim 0.5$  mm). A droplet was placed on a CRA-CM-modified plate (A), followed by UV light irradiation at

the right edge of the droplet to cause an asymmetrical spreading (B). Subsequent irradiation with blue light at the left edge resulted in dewetting, leading to the displacement of the droplet (C). The repetition of this stepwise photoirradiation resulted in the approach of the droplet to the bead (D), which was finally captured by the liquid (E). **Fig. 6 (right).** Light-driven displacement of an NPC-02 droplet in a glass tube. A droplet of NPC-02 was placed in the tube (A), and one edge of the droplet was exposed to UV light, leading to the slight advancement of the droplet (B). Subsequent irradiation with blue light at the opposite edge pushed the droplet to the left (C).

taining surfactants can be controlled by light (26). In contrast, our work demonstrates a photoinduced liquid motion triggered by azobenzenes immobilized on a solid surface.

15. S.-K. Oh, M. Nakagawa, K. Ichimura, *Chem. Lett.* **4**, 349 (1999).
16. M. Fujimaki *et al.*, *Langmuir* **14**, 4495 (1998).
17. E. Kurita *et al.*, *J. Mater. Chem.* **8**, 397 (1998).
18. Olive oil is a mixture containing fatty acids, vitamins and so on, and contains 55 to 85% oleic acid.
19. Y. L. Chen, C. A. Helm, J. N. Israelachvili, *J. Phys. Chem.* **95**, 10736 (1991).
20. The condition includes both equilibrium thermody-

amic and dynamic factors, and is applicable to previously described methods for moving liquids by a driving force arising from an imbalance in surface tension forces. As an example, see (5).

21. An NPC-02 drop at 40°C (nematic-isotropic transition temperature of NPC-02 is 35°C) also exhibited the light-driven motion. Detailed studies including the effect of liquid crystallinity on the spreading kinetics of the liquid will be published elsewhere [S.-K. Oh, M. Nakagawa, K. Ichimura, in preparation].
22. T. Seki, H. Sekizawa, S. Morino, K. Ichimura, *J. Phys. Chem. B* **102**, 5313 (1998).

23. I. Panaiotov, S. Taneva, A. Bois, F. Rondelez, *Macromolecules* **24**, 4250 (1991).
24. F. Brochard, *Langmuir* **5**, 432 (1989).
25. The difference between the advancing and receding dynamic contact angles was less than 2°, even though the advancing and receding edges of the moving droplet would be placed on cis-rich ( $\theta_{\text{adv}}^{\text{cis}} = 11^\circ$ ) and trans-rich ( $\theta_{\text{adv}}^{\text{tr}} = 24^\circ$ ) surfaces, respectively.
26. J. Y. Shin and N. L. Abbott, *Langmuir* **15**, 4404 (1999).

21 January 2000; accepted 30 March 2000

## Raman Spectroscopy of Iron to 152 Gigapascals: Implications for Earth's Inner Core

Sébastien Merkel,<sup>1,2</sup> Alexander F. Goncharov,<sup>1</sup> Ho-kwang Mao,<sup>1</sup> Philippe Gillet,<sup>2</sup> Russell J. Hemley<sup>1</sup>

Raman spectra of hexagonal close-packed iron ( $\epsilon$ -Fe) have been measured from 15 to 152 gigapascals by using diamond-anvil cells with ultrapure synthetic diamond anvils. The results give a Grüneisen parameter  $\gamma_0 = 1.68 (\pm 0.20)$  and  $q = 0.7 (\pm 0.5)$ . Phenomenological modeling shows that the Raman-active mode can be approximately correlated with an acoustic phonon and thus provides direct information about the high-pressure elastic properties of iron, which have been controversial. In particular, the  $C_{44}$  elastic modulus is found to be lower than previous determinations. This leads to changes of about 35% at core pressures for shear wave anisotropies.

Understanding recent geophysical observations of elastic anisotropy, possible superrotation, and magnetism of Earth's inner core (1) requires detailed information about the

thermodynamic and elastic properties of core-forming materials under appropriate conditions. High-pressure properties of iron are crucial in this respect because the core is

composed primarily of this element. Iron transforms from the body-centered cubic (bcc) phase ( $\alpha$ -Fe) at ambient conditions to a face-centered cubic (fcc) phase ( $\gamma$ -Fe) at moderate pressures and temperatures and to a higher-pressure hexagonal close-packed (hcp) phase ( $\epsilon$ -Fe) ( $>13$  GPa) (2). The hcp phase has a wide stability field to more than 300 GPa and high temperatures (3–5). Techniques to measure lattice strains at megabar pressures (6) have determined the elastic properties of  $\epsilon$ -Fe to 210 GPa (7). These results show discrepancies with calculations in which first-principles methods were used (8–10), in particular for shear moduli and anisotropy. Measurements and estimates of the Grüneisen parameter, an important thermodynamic property of iron that relates the

<sup>1</sup>Geophysical Laboratory and Center for High Pressure Research, Carnegie Institution of Washington, 5251 Broad Branch Road, NW, Washington, DC 20015, USA. <sup>2</sup>Laboratoire des Sciences de la Terre, UMR CNRS 5570, Ecole Normale Supérieure de Lyon, 46 allée d'Italie, 69364 Lyon Cedex 07, France.